

CartoMapQA: A Fundamental Benchmark Dataset Evaluating Vision-Language Models on Cartographic Map Understanding

Huy Quang Ung
xhu-ung@kddi.com
KDDI Research, Inc.
Fujimino, Japan

Guillaume Habault
xgu-habault@kddi.com
KDDI Research, Inc.
Fujimino, Japan

Yasutaka Nishimura
yu-nishimura@kddi.com
KDDI Research, Inc.
Fujimino, Japan

Hao Niu
ha-niu@kddi.com
KDDI Research, Inc.
Fujimino, Japan

Roberto Legaspi
ro-legaspi@kddi-research.jp
KDDI Research, Inc.
Fujimino, Japan

Tomoki Oya
to-ooya@kddi.com
KDDI Research, Inc.
Fujimino, Japan

Ryoichi Kojima
ry-kojima@kddi.com
KDDI Research, Inc.
Fujimino, Japan

Masato Taya
ma-taya@kddi.com
KDDI Research, Inc.
Fujimino, Japan

Chihiro Ono
ci-ono@kddi.com
KDDI Research, Inc.
Fujimino, Japan

Atsunori Minamikawa
at-minamikawa@kddi.com
KDDI Research, Inc.
Fujimino, Japan

Yan Liu
yanliu.cs@usc.edu
University of Southern
California
Los Angeles, USA

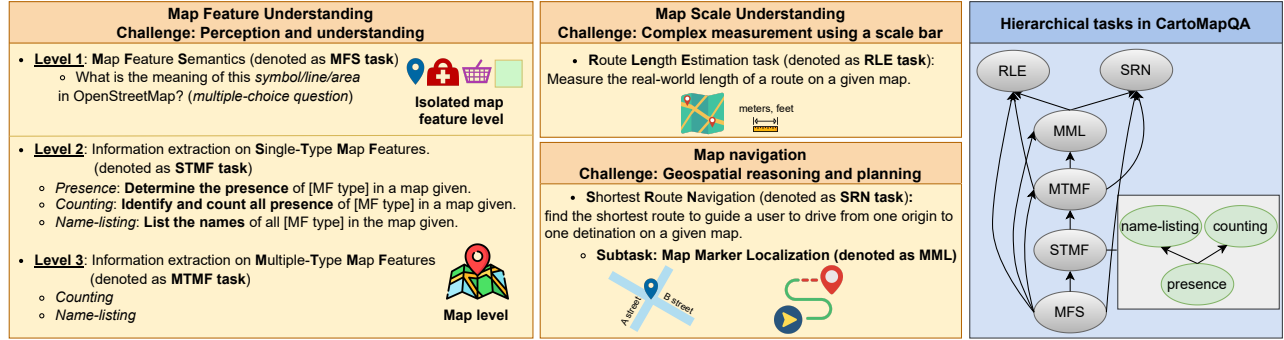


Figure 1: Overview of CartoMapQA, a benchmark designed to evaluate Large Visual-Language Models on cartographic map understanding, including Map Feature recognition, map scale interpretation, and turn-by-turn navigation. It consists of six hierarchically structured tasks, where lower-level tasks serve as foundation for more complex, higher-level ones.

Abstract

The rise of Visual-Language Models (LVLMs) has unlocked new possibilities for seamlessly integrating visual and textual information. However, their ability to interpret cartographic maps remains largely unexplored. In this paper, we introduce CartoMapQA, a benchmark specifically designed to evaluate LVLMs’ understanding of cartographic maps through question-answering tasks. The dataset includes over 2000 samples, each composed of a cartographic map, a question (with open-ended or multiple-choice answers), and a ground-truth answer. These tasks span key low-, mid- and high-level map interpretation skills, including symbol recognition, embedded information extraction, scale interpretation, and route-based reasoning. Our evaluation of both open-source and proprietary LVLMs reveals persistent challenges: models frequently struggle with map-specific semantics, exhibit limited geospatial reasoning, and are prone to Optical Character Recognition (OCR)-related errors. By isolating these weaknesses, CartoMapQA offers

a valuable tool for guiding future improvements in LVLM architectures. Ultimately, it supports the development of models better equipped for real-world applications that depend on robust and reliable map understanding, such as navigation, geographic search, and urban planning. Our source code and data are openly available to the research community at:

<https://github.com/ungquanghuy-kddi/CartoMapQA.git>

CCS Concepts

• **Applied computing** → **Cartography**; • **Computing methodologies** → **Computer vision**; **Machine learning**; *Information extraction*.

Keywords

Benchmark dataset, cartographic map understanding, evaluation, vision-language models, map features, map scales, navigation

1 Introduction

Recent advancements in Large Language Models (LLMs) and Large Visual-Language Models (LVLMs) have demonstrated remarkable generalization and reasoning capabilities across a variety of domains, including programming [22], mathematical reasoning [2], Visual Question Answering (VQA) [31], and common sense reasoning [45]. More recently, there has been growing interest in leveraging LLMs and LVLMs for geospatial applications [7, 14, 20, 37, 44], with work spanning both model development [7, 33, 52] and the construction of specialized benchmarks [15, 17, 32, 53]. These efforts target key tasks such as object recognition [17], counting [55], and geospatial reasoning, including social indicator estimation [33, 52] and location-based information retrieval [15]. Despite their promise, existing approaches often rely on text descriptions or satellite imagery [26, 52], each with critical limitations. Textual data is constrained by token limits and typically lacks the spatial richness needed for detailed geospatial reasoning. Satellite imagery, while rich in visual detail, frequently includes irrelevant elements—such as foliage or architectural variation—that may distract models from the task at hand.

Cartographic Maps (CMs) present a compelling alternative. Like satellite imagery, they offer spatially grounded visual input, but in a more structured and abstracted form. Using standardized symbols, color-coded regions, and textual labels, CMs provide a simplified yet information-rich view of geographic data—making them especially well suited for LVLMs to reason about spatial relationships, landmarks, distances, and navigation. Recently, Dihan et al. [15] has evaluated Multi-modal Large Language Models (MLLMs) using CMs, however their benchmark focused mainly on user-level complex tasks, limiting potential insight into foundational limitations of LVLMs. Moreover, their experiments with visual inputs—based on proprietary *Google Maps* imagery—showed lower performance compared to selective textual context or API inputs, underscoring the difficulty of map-based reasoning.

In this paper, we present CartoMapQA, a benchmark dataset specifically designed to evaluate LVLMs’ ability to interpret and reason over cartographic maps through a structured set of question-answering tasks. Figure 1, CartoMapQA defines three objectives: (1) **Map Feature Understanding**: Identify (Map Feature Semantics (MFS) task), detect, count, and associate Map Feature (MF) with corresponding labels (Single-Type Map Feature (STMF) and Multiple-Type Map Feature (MTMF) tasks). (2) **Map Scale Understanding**: Locate the scale notation, identify pre-defined routes, measure route length and compute real-world distances between map markers (Route Length Estimation (RLE) task). (3) **Map Navigation**: Comprehend direction, determine the shortest drivable route between map markers and describe turn-by-turn navigation (Shortest Route Navigation (SRN) task), with supporting evaluation on marker localization accuracy (Map Marker Localization (MML) task). The dataset consists of 2251 questions across 853 maps sourced from *OpenStreetMap* [40] across three English-speaking countries, ensuring that language comprehension does not influence the evaluation. We adopt *OpenStreetMap*’s definition of MF—any element represented by a symbol, line, or colored area, possibly with a textual label such as Point of Interests (POIs), roads, or land-use areas.

To assess model capabilities with cartographic maps, we evaluate various LVLMs in a zero-shot setting. Our findings include: While detailed results are presented in the subsequent sections, our findings include:

- While proprietary models like *Gemini 2.5 Pro* [13], *OpenAI o1* [25], and *o3* [39] achieved top scores, across all tasks, their performance is still limited.
- Open-source models generally underperform across most tasks, with significant performance gaps in higher-level reasoning tasks.
- In both STMF and MTMF tasks, models often correctly associate MFs with their textual labels. Error analysis reveals minimal hallucination, with most failures stemming from Optical Character Recognition (OCR) error or the incorrect association of a MF with a semantically related type (e.g., restaurant vs. fast-food).
- In RLE, a review of *o1*’s answers on some samples shows promising results but with irregular behaviors.
- SRN remains particularly challenging; the best-performing LVLM, *o3*, correctly identifies the shortest route in only 33% of samples, and just 37% of its answers successfully connect the map markers—exposing critical limitations in geospatial reasoning and planning.

Our task design further reveals a hierarchical, i.e., a foundational or prerequisite, dependence. Specifically, the ability to perform higher-level reasoning depends on the prior availability of low-level map understanding. In fact, models that struggle with basic symbol identification are unlikely to succeed in measurement or navigation tasks. Some models exhibit modality-specific strengths, compensating for visual weaknesses through stronger textual-based reasoning.

CartoMapQA provides a comprehensive framework for evaluating and advancing LVLMs in map-based reasoning, offering both a foundation for future extensions and a critical tool for diagnosing current limitations. With practical applications in navigation, urban planning, tourism, and real estate, CartoMapQA also lays essential groundwork for building next-generation LVLMs capable of advance geospatial reasoning. **Our contributions** are as follows:

- We introduce CartoMapQA, the first hierarchically structured benchmark specifically designed to assess LVLMs’ cartographic map understanding across three core objectives: visual recognition, spatial measurement, and navigation.
- We evaluate 15 LVLMs, including cutting-edge proprietary models, and offer detailed analysis of their performance and failure cases.
- We demonstrate CartoMapQA’s utility in exposing current model limitations and guiding future improvements in architecture and training for geospatial reasoning.

2 Related works

This section provides an overview of prior research on LLMs in spatial understanding and geospatial tasks, recent developments in LVLMs, and benchmark datasets for geospatial analysis.

2.1 LLMs for spatial understanding

Spatial understanding is crucial for accurate map interpretation. Yet, recent studies demonstrate that current language-only LLMs struggle with several tasks and especially relatively simple spatial tasks that would appear trivial for humans. Such tasks include navigating two-dimensional grids to reach a target [46], reasoning about cardinal directions in contextual scenarios [12], interpreting spatial relationships (visual correspondence, depth perception, object perception, and movement) across multi-frame scene [50]; and solving spatial tasks involving complex structures [51], such as hexagonal grids, rings, and trees. Such outcomes underscore the inherent challenges of performing spatial reasoning using language-only LLMs. This also highlights the potential of incorporating additional modalities, particularly visual inputs, to enhance the geospatial reasoning capabilities of the models.

2.2 LLMs and LVLMs for geospatial tasks

Recent research has explored the extent to which LLMs possess implicit geospatial knowledge. Some studies have evaluated language-only LLMs on tasks such as Geographic Information Systems (GIS) exams [37] and specific geospatial test cases [44]. These studies reveal that while these models exhibit partial understanding, they also make frequent errors. Manvi et al. [33] fine-tuned *GPT-3.5* with custom prompts for estimating population density and found that, despite its limitations, the model displayed a notable level of geospatial awareness. Similarly, Bhandari et al. [7] acknowledged the potential of language-only LLMs in geospatial applications but emphasized the need for further enhancement. Collectively, these works underscore the limitations of language-only LLMs and the need for improved geospatial understanding, e.g., using MLLMs.

Despite their potential, few LVLMs have been specifically developed for geospatial tasks. GeoChat, introduced by Kuckreja et al. [26], was the first LVLM to offer multitask conversational capabilities on remote sensing data, covering several tasks such as object recognition and counting. Yan et al. [52] proposed a model that combines satellite imagery and textual data via contrastive learning to profile urban regions and predict spatial indicators as well as other prompt-guided tasks. These efforts show that combining visual and textual modalities are particularly well-suited for advancing cartographic and geospatial understanding.

2.3 Pre-trained large visual-language models

Recent advances in LVLMs have significantly accelerated progress toward general-purpose AI systems capable of processing and reasoning over both visual and textual inputs.

Proprietary LVLMs: The release of ChatGPT [38], demonstrating unprecedented abilities in understanding, reasoning, and generating text across a broad range of tasks, sparked intense interest in developing commercial models even more efficient. Leading proprietary LVLMs include *OpenAI o1* [25], *o3* [39], *Gemini 2.5 Pro* [13], and *Claude 3.7 Sonnet* [4], which demonstrate extended thinking features. These models are positioned as general-purpose models with ambitions toward Artificial General Intelligence (AGI).

Open-source LVLMs: Open-source LVLMs have greatly influenced the AGI landscape by democratizing multimodal research—especially, visual and textual data—enabling rapid innovation and

reproducibility. Over the past two years, several open-source models have gained prominence, including the *LLaVA* series [27, 28, 30, 31], *Llama* series [19, 34, 35], *MiniGPT-4* [56], *VisionLLM* [47], *Qwen-VL* [5, 6], *CogVLM* [23, 48], *InternVL* [9–11], and many others [3, 18, 29, 41]. These models continue to advance the boundaries of visual-language understanding.

However, despite their impressive performance across various benchmarks and tasks, these proprietary and open-source models have not yet been fully evaluated on CM interpretation tasks.

2.4 Benchmark datasets for geospatial tasks

Most benchmark datasets for geospatial tasks rely heavily on satellite or street-view imagery as visual inputs. Lobry et al. [32] introduced *RSVQA*, a VQA dataset based on remote sensing data, targeting tasks such as object presence detection, counting, and classification. Yang et al. [53] proposed a platform that allows agents to interact with virtual environments constructed from street-view images, enabling the evaluation of LVLMs on tasks like place recognition and VQAs. For urban environments, CityBench [17] provides a simulator-based evaluation tool, using satellite or street-view images, to assess LLMs’ performance on a wide range of urban tasks—from perception and understanding to decision-making. In addition, Zhang et al. [55] is conducting ongoing analysis of *GPT-4V*’s capabilities on spatial understanding based on satellite imagery. While these studies demonstrate the potential of LVLMs in geospatial tasks, they also expose persistent limitations such as modality dominance (e.g., prioritizing textual over visual inputs) and geospatial biases (e.g., performing better in well-known locations).

To evaluate more directly map-based spatial reasoning, Dihan et al. [15] recently introduced the MapEval dataset, which uses digital map views from *Google Maps*. Their tasks, framed as multiple-choice questions, center on user-oriented applications such as extracting place information, identifying the nearest POI, and routing. While MapEval tests different input modalities (text, API, visual), it lacks fine-grained, low-level map interpretation tasks, limiting its diagnostic power in revealing foundational weaknesses of LVLMs in CM understanding. Its reliance on multiple-choice formats further restricts insight into model reasoning, and the small number of questions per task may hinder generalizability.

In contrast, CartoMapQA introduces a specifically designed benchmark that spans a hierarchy of tasks—from basic MF recognition to advanced reasoning such as scale interpretation and navigation. Importantly, we introduce a dedicated task for interpreting scale bars and estimating real-world distances—an essential yet under-explored capability for practical geospatial applications. The open-ended nature of most of our questions better reflects real-world use cases and allows for deeper insight into model behaviors, including hallucinations and reasoning failures. Moreover, our benchmark evaluates recent proprietary and open-source models, offering a more current and thorough understanding of the state of the field. A comparison with MapEval is presented in Table 1.

Table 1: Comparison between CartoMapQA and MapEval. MC stands for multiple-choices. * Include information retrieval testing, while ** evaluate insufficient context detection ability, which are not fully CM-related.

	Task level			Number of questions	Answer format
	Low	Mid	High		
MapEval [15]	X	Counting Place Info*	Nearby, Routing Trip, Unanswerable**	700	MC (100%)
CartoMapQA (ours)	MFS	STMF, MTMF, MML	RLE, SRN	2251	Open-ended (79%) MC(21%)

Table 2: Key statistics of CartoMapQA.

Statistics	Number
Total questions:	2251
*MFS : STMF : MTMF : RLE : MML : SRN	463 : 510 : 150 : 600 : 250 : 278
Multiple-choice questions:	
*MFS	463 (21%)
Open-ended questions:	
*STMF, MTMF, RLE, MML, and SRN	1788 (79%)
Total OpenStreetMap maps:	853
*San Jose : Manchester : Melbourne	324 : 297 : 232
*(STMF / MTMF) : RLE : MML : SRN	150 : 300 : 125 : 278
Zoom-in levels: (level 19 is the most zoom-in level)	
15 : 16 : 17 : 18 : 19	1 : 7 : 213 : 187 : 445
Map’s size: (width × height)	1366 × 768 pixels

3 The CartoMapQA dataset

3.1 Overview of CartoMapQA

Our dataset is designed to evaluate LVLs on three core objectives: (i) map information understanding, (ii) scale and distance interpretation, and (iii) directional reasoning. Key statistics are summarized in Table 2 and visual examples are shown in Figure 2.

Map Feature Semantics (MFS): This task evaluates LVLs’ ability to recognize isolated Map Features (MFs), without contextual cues from a full cartographic map. It provides 463 multiple-choice

questions, each tied to a unique MF image and offering five candidate answers with a single correct option. This task is composed of all MFs provided in *OpenStreetMap*¹. MFS tests foundational semantic understanding of cartographic MF images.

Single-Type Map Feature (STMF): The goal of this task is to test LVLs’ ability to detect, classify and analyze a single type of MF in full cartographic maps. We randomly selected three major cities from different countries: San Jose (USA), Manchester (UK), and Melbourne (Australia). STMF includes 150 CMs (50 per city), all sourced from *OpenStreetMap*. Each one is rendered at the finest *zoom-in level* (i.e., 19) to include finest details, such as POIs. To comprehensively evaluate this task, we define three requests: (1) presence: Determines whether the model can detect and identify at least one instance of a target MF type; (2) counting: Assesses the model’s ability to accurately identify and count all instances of a given MF type; and, (3) name-listing: Establishes whether the model can correctly extract the textual labels associated with the target MF type. STMF covers 22 usual MF types, including *restaurants*, *convenient stores*, and *parking lots*. Therefore, each CM is associated with several questions, resulting in a total of 510 questions for this task. The list of these MFs is provided in Table 9 (Appendix A). This framework progressively judges the model’s visual detection accuracy, classification, label-association, and basic counting skills.

Multiple-Type Map Feature (MTMF): Building on STMF, this task examines the LVLs’ counting and name-listing abilities across multiple types of MFs simultaneously within a single CM. MTMF uses the same CMs as STMF and focuses on the same 22 MF types. This results in a total of 150 questions for this task. MTMF specifically tests the multitasking capability of LVLs, establishing a foundation for complex inference tasks that require the ability to interpret and understand information—potentially overlapping—for instance, when analyzing and describing CMs.

¹https://wiki.openstreetmap.org/wiki/OpenStreetMap_Carto/Symbols

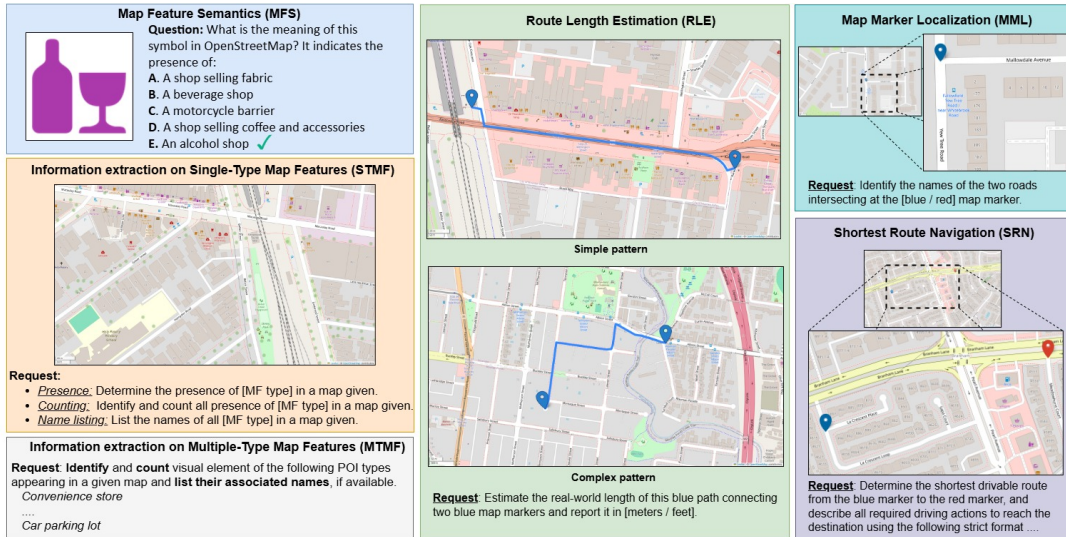


Figure 2: Examples of questions and requests featured in CartoMapQA. Note: these are short versions of the actual questions and requests used in the dataset, which can be found in the implementation repository.

Route Length Estimation (RLE): This task evaluates LVLMS’ ability to interpret scale bars and estimate real-world length of predefined routes in meters or feet. RLE includes 300 CMs (from the same three cities) rendered at *zoom-in levels* ranging from 15 to 19. As illustrated in Figure 2, each cartographic map includes two blue map markers connected by a predefined blue path and a visible scale bar providing a visual indication of distance in both meters and feet. Two difficulty levels are defined: (1) Simple: Straightforward paths with few turns; (2) Complex: Longer paths with multiple turns. RLE is crucial for assessing scale awareness, a valuable benchmark for advanced LVLMS applications like navigation, planning, or proximity-based services (e.g., nearest POIs). The distribution of route lengths is shown in Figure 6 (Appendix A).

Shortest Route Navigation (SRN): This task tests LVLMS in terms of directional awareness, finding the shortest route and turn-by-turn navigation. It is achieved by prompting the model to generate turn-by-turn instructions for the shortest drivable route between two markers on a CM: a blue marker (origin) and a red marker (destination). We generated 278 valid routes across the three cities (originally 300; some were filtered out due to readability issues, e.g., overlapping elements), on CMs rendered at *zoom-in levels* ranging from 17 to 19. For simplicity, we assume the user is seated in a vehicle which is oriented toward the top of the CM, at the starting marker. To standardize outputs, we instruct models to use a structured navigation format: *[blue, <action₁>, road₁, <action₂>, road₂, ..., <action_n>, road_n, red]*, where each *action_i* belongs to one of four categories of directional change: *continue straight*, *make a U-turn and continue straight*, *turn left*, and *turn right*. For instance, if the shortest route involves making a U-turn at the start, followed by driving on “Main Street”, a left turn onto “2nd Avenue”, and a right turn onto “Elm Street” to reach the destination, the response should be: *[blue, make a U-turn and continue straight, Main Street, turn left, 2nd Avenue, turn right, Elm Street, red]*. This format aligns closely with commercial navigation systems (e.g., *Google Maps*) and supports consistent evaluation. The distribution of the number of steps (excluding the origin point) in our generated routes is presented in Figure 7 (Appendix A). Beyond its central role in navigation systems, SRN provides the foundation for more complex applications such as trip planning.

It is worth noting that in both RLE and SRN, we employ dedicated map markers to designate the origin and destination points—rather than relying on existing POIs. This design choice simplifies the task and minimizes errors that might originate from models’ potential inability to detect, classify or associate label with POIs. Nevertheless, this approach requires to specifically evaluate the models’ detection capability of such dedicated map markers.

Map Marker Localization (MML): This task evaluates LVLMS’ ability to localize a colored map marker within a cartographic map. MML is essential as map markers are commonly utilized to mark specific locations on a CM. Assessing LVLMS’ capability on such a task is then of crucial importance. Rather than asking models for exact coordinates—which can introduce ambiguity—we restrict the position of markers at the intersection of two named roads. The model is then prompted to report the names of these intersecting roads. Linking marker locations to the identification of road names not only simplifies the annotation process but also aligns directly with the requirements of our SRN task.

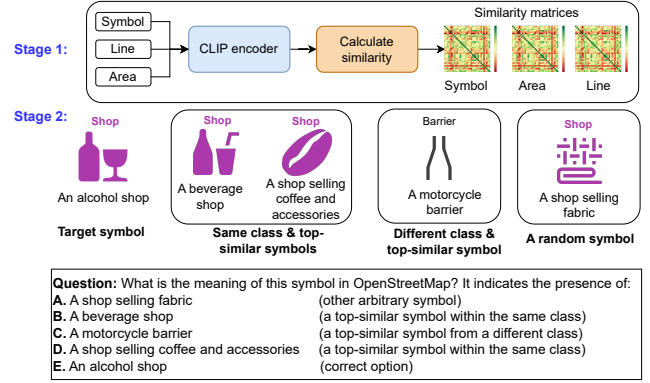


Figure 3: Illustration of the process used to generate answer choices for the multiple-choice questions in the MFS task.

3.2 Cartographic map generation

While well-known platforms such as *Google Maps* and *Apple Maps* provide cartographic maps that are widely used, their strict and restrictive data-sharing policies^{2 3} limit their suitability for an open dataset. To ensure that CartoMapQA remains fully accessible to the research community, we adopt *OpenStreetMap* as our CMs rendering platform. CMs in CartoMapQA are generated using the *Folium* Python package [42], which allows for interactive map rendering and supports built-in *OpenStreetMap* tilesets. For tasks involving path planning—specifically, RLE and SRN—we utilize *OSMnx* [8] and *NetworkX* [21] packages to compute and visualize paths, including shortest routes, between two points. These tools enable precise path calculations and ensure faithful representation of MFs, maintaining spatial and semantic fidelity throughout the dataset.

3.3 Answer preparation

MFS: To test a model’s ability to distinguish the correct answer from distractors and unrelated choices, we design a method leveraging the CLIP encoder [43], as illustrated in Figure 3.

First, we compute embeddings for all MF images using CLIP and then, generate pairwise Euclidean-distance similarity matrices separately for each MF category: symbol, line and area. Given that *OpenStreetMap* provides semantic classifications for each MF (e.g., shop, amenity, barrier, etc.), we use such classifications alongside the similarity matrices to select distractors based on three criteria: (1) Two most similar MFs from the same class as the correct answer. (2) One most similar MF from a different class. (3) One randomly selected MF. The labels associated with these MFs, combined with the correct label, form the five choices in each multiple-choice question. Finally, to prevent positional bias, we randomly shuffle options’ order, ensuring that the correct answer appears in a uniformly distributed position.

STMF and MTFM: We extracted MF data within each CM’s boundaries directly from *OpenStreetMap*. To ensure accuracy and consistency between the extracted data and what is visually represented on the rendered CMs, a human annotator manually verified

²<https://cloud.google.com/maps-platform/terms#3.-license>

³<https://www.apple.com/legal/internet-services/maps/terms-en.html>

the counts and names of all MFs. This validation step helps eliminate discrepancies that may arise due to rendering limitations, outdated entries, or label mismatches between *OpenStreetMap* data and the actual content displayed in the CMs.

RLE, MML and SRN: Ground-truth for these tasks were obtained using *NetworkX* and *OSMnx*, ensuring accurate and consistent spatial reasoning based on real-world geography. For RLE, the true distance was computed using the geographic coordinates (latitude and longitude) of the start and end markers of the predefined path. For MML, we randomly selected graph nodes positioned at the intersection of two roads within a selected area of each CM. The names of these intersecting roads were then extracted to form the correct answer. For SRN, we extracted the shortest drivable path as an ordered sequence of graph nodes. This sequence was then translated into our standardized turn-by-turn route format by mapping consecutive node pairs to their respective road names and inferring the required directional change. Finally, all generated routes were manually verified and corrected to ensure alignment with the visual content of each CM.

Table 3: Main results of the Map Feature Semantics (MFS) task. Bold and underlined values indicate the best and second-best performance, respectively, within each group of models.

Model	Acc. (↑)			
	Symbol	Area	Line	Overall
<i>Random baseline</i>	0.173	0.222	0.232	0.194
LLama 3.2 11B	0.507	0.326	0.222	0.415
InternVL 2.5 8B	0.410	0.168	0.189	0.317
LLaVa-OV 7B	0.655	0.221	0.311	0.499
Qwen-VL 2.5 7B	0.597	0.284	0.311	0.477
LLama 4 Scout	0.590	0.316	0.311	0.479
LLama 3.2 90B	0.608	0.316	0.267	0.482
InternVL 2.5 78B	0.637	0.295	0.267	0.495
LLaVa-OV 72B	0.683	0.263	0.233	0.510
Qwen-VL 2.5 72B	0.662	0.316	0.256	0.512
GPT-4(V)	0.669	0.253	0.300	0.512
GPT-4o	0.723	0.232	0.444	0.568
o1	0.777	0.368	0.356	0.611
o3	0.806	0.379	0.378	0.635
Gemini 2.5 Pro	0.820	0.389	0.411	0.652
Claude 3.7 Sonnet	0.687	0.305	0.356	0.540

4 Experiments

Using CartoMapQA, we evaluate various emerging LVLMs, including both open-source and proprietary models, under a zero-shot setting to assess their ability to understand cartographic maps without prior fine-tuning. For each task, we design a tailored prompt which includes output formatting instructions to streamline response processing. Due to space constraints, full prompt templates are provided in our implementation source code⁴. All experiments were conducted on four NVIDIA A100 GPUs with 80GB of memory.

4.1 Baselines

From the LVLMs introduced in subsection 2.3, we evaluate five recent open-source models that rank among the top performers on the multi-discipline college-level MMMU benchmark [54]. For each, we include both a lightweight and a large-scale variant: (1) *InternVL 2.5* (8B/78B) [9], (2) *Qwen-VL 2.5* (7B/72B) [6], (3) *LLaVa-OV* (7B/72B) [28], (4) *LLama 3.2* (11B/90B) [16, 34, 35], and (5) *LLama 4 Scout* (109B) [36], a Mixture-of-Experts model with only 17B parameters activated in the inference phase.

In addition, we test six famous proprietary models: (1) *GPT-4V* [1] (gpt-4-turbo-2024-04-09), (2) *GPT-4o* [24] (gpt-4o-2024-08-06), (3) *OpenAI o1* [25] (o1-2024-12-17), (4) *o3* [39] (o3-2025-04-16), (5) *Gemini 2.5 Pro* [13] (gemini-2.5-pro-preview-03-25), and (6) *Claude 3.7 Sonnet* [4] (claude-3-7-sonnet-20250219). Finally, for MFS, STMF and MTMF tasks, we include a *Random* baseline, which selects answers randomly, to establish a lower-bound reference for model performance.

4.2 Evaluation process

We evaluate LVLm responses using task-specific metrics tailored to each question or request. For multiple-choice questions (MFS), accuracy (Acc.) is used to measure the proportion of correct answers. Presence requests (STMF) are assessed using both accuracy (Acc.) and macro-average F1-score (MF1) to capture class-wise balance. Answers to the counting requests (STMF, MTMF) are evaluated using both Root Mean Squared Error (RMSE) and the coefficient of determination (r^2). Name-listing requests (STMF, MTMF) are

⁴<https://github.com/ungquanhuy-kddi/CartoMapQA.git>

Table 4: Main results of the Single-Type Map Feature (STMF) task. Bold and underlined values indicate the best and second-best performance, respectively, within each group of models.

Model	Presence		Counting		Name listing		
	Acc. (↑)	MF1 (↑)	RMSE (↓)	r^2 (↑)	aPrec. (↑)	aRec. (↑)	aF1 (↑)
<i>Random baseline</i>	0.487	0.486	7.278	-5.764	-	-	-
LLama 3.2 11B	0.597	0.530	2.590	0.143	0.305	0.492	0.342
InternVL 2.5 8B	0.707	0.706	2.662	0.095	0.427	0.482	0.407
LLaVa-OV 7B	0.754	0.752	1.923	0.528	0.365	0.372	0.340
Qwen-VL 2.5 7B	0.691	0.680	2.270	0.342	0.710	0.615	0.624
LLama 4 Scout	0.785	0.784	2.398	0.266	0.678	0.726	0.663
LLama 3.2 90B	0.749	0.746	2.322	0.312	0.556	0.595	0.542
InternVL 2.5 78B	0.733	0.730	1.729	0.618	0.544	0.547	0.519
LLaVa-OV 72B	0.743	0.736	1.999	0.490	0.580	0.556	0.537
Qwen-VL 2.5 72B	0.728	0.716	2.166	0.401	0.753	0.744	0.706
GPT-4(V)	0.738	0.738	2.240	0.359	0.737	0.695	0.687
GPT-4o	0.780	0.775	1.710	0.626	0.850	0.839	0.821
o1	0.785	0.774	1.812	0.581	0.824	0.829	0.813
o3	0.801	0.797	1.789	0.592	0.856	0.868	0.847
Gemini 2.5 Pro	0.843	0.842	1.367	0.761	0.885	0.929	0.894
Claude 3.7 Sonnet	0.801	0.798	1.717	0.624	0.739	0.737	0.714

judged based on average precision (aPrec.), average recall (aRec.), and average F1-score (aF1), computed across all requests. For the estimation of real-world route length (RLE), the estimated length is compared to the ground-truth and evaluated using RMSE, Mean Absolute Percentage Error (MAPE), and r^2 . For map marker localization (MML), the ability to correctly identify both road names at the marker’s location is measured with accuracy (Acc.). For the SRN task, we employ the following metrics:

- Shortest Route Success Rate (denoted as SR^2): Proportion of the route generated by the model that exactly match the ground-truth shortest route.
- Average Step Accuracy (denoted as aSA): This metric quantifies how much the route generated by the model overlay with the ground-truth shortest route. For each route, let L be the total number of steps in the true shortest route excluding the starting point and k the length of the longest matching prefix of the model’s generated steps. For example, if the true shortest route is *[blue, Main Street, turn right, 2nd Avenue, red]* and the generated route is *[blue, Main Street, turn right, Main Avenue, red]*, then $L = 4$ (total steps without “blue”) and $k = 2$ (only “Main Street” and “turn right” match the ground truth after the starting point). The step accuracy is then defined as k/L , and aSA is the mean across all routes.
- Connectivity: Proportion of the route generated by the model to form a continuous path from origin to destination, regardless of real-world traffic constraints (e.g., one-way streets). This metric evaluates the model’s ability to produce a route connecting two map markers.

To streamline the evaluation process, we developed a workflow for extracting key information from model responses. In cases of invalid or missing answers in multiple-choice or binary requests, these are replaced with a randomly selected option (similar to [54]); with counting requests, we substitute them with a random number within a predefined range; and invalid answers in name-listing requests are replaced by an empty list. However, such fallbacks were rarely needed in our experiments.

4.3 Main results

Map Feature Semantics (MFS): Table 3 lists the results for this task. When considering all MFs collectively (the ‘Overall’ column), all models substantially outperform the *Random* baseline, with *Gemini 2.5 Pro* achieving the highest accuracy, closely followed by *o3*. Among open-source models, *Qwen-VL 2.5 72B* ranks highest, whereas *InternVL 2.5 8B* scores the lowest. The performance gap between lightweight and large-scale open-source models is relatively small, but the difference between large-scale open-source and advanced proprietary models is more significant. When analyzing the performance per MF category (symbol, line or area columns), models perform similarly—and generally poorly—on line and area MFs, indicating limited interpretive ability in these categories. In contrast, performances on symbol reveal a clearer performance separation between models. These findings suggest that while current models can, to some extent, interpret MFs when isolated from any contextual information, substantial room for improvement remains,

particularly for open-source models and on MF categories requiring more precise understanding.

Table 5: Main results of the Multiple-Type Map Feature (MTMF) task. Bold and underlined values indicate the best and second-best performance, respectively, within each group of models.

Model	Counting		Name listing		
	aRMSE (↓)	ar^2 (↑)	amPrec. (↑)	amRec. (↑)	amF1 (↑)
<i>Random baseline</i>	8.345	-323.447	-	-	-
LLama 3.2 11B	0.919	-0.168	0.315	0.217	0.239
InternVL 2.5 8B	1.285	-6.100	0.169	<u>0.414</u>	0.200
LLaVa-OV 7B	1.131	<u>-2.290</u>	0.126	0.236	0.133
Qwen-VL 2.5 7B	<u>1.032</u>	-2.408	<u>0.295</u>	0.614	0.351
LLama 4 Scout	0.833	-2.135	<u>0.431</u>	<u>0.626</u>	<u>0.457</u>
LLama 3.2 90B	0.968	-2.282	0.407	0.419	0.341
InternVL 2.5 78B	<u>0.825</u>	-1.575	0.318	0.560	0.355
LLaVa-OV 72B	0.826	-0.180	0.299	0.373	0.271
Qwen-VL 2.5 72B	0.686	-0.329	0.566	0.655	0.556
GPT-4(V)	0.840	-0.587	0.434	0.561	0.425
GPT-4o	0.717	0.058	0.533	0.705	0.550
o1	<u>0.593</u>	0.290	0.691	0.797	0.712
o3	0.612	<u>0.217</u>	0.566	<u>0.846</u>	0.644
Gemini 2.5 Pro	0.582	0.001	<u>0.587</u>	0.888	<u>0.668</u>
Claude 3.7 Sonnet	0.662	-0.844	0.414	0.696	0.469

Single-Type Map Feature (STMF): Table 4 reports the results across the three evaluated requests. Overall, most models substantially outperform the *Random* baseline. It is important to note that, for the counting request, the *Random* baseline selects a number at random between $[0, N]$, with $N = 16$ representing the maximum number of a single-type MF observed in our dataset. Proprietary models overall exhibit superior performance, with once again *Gemini 2.5 Pro* achieving the highest performance across all request types. Among open-source models, no single model consistently performs the best overall; performance is mostly task-specific. For instance, *Qwen-VL 2.5* excels for name-listing.

In the presence request, top models from the different groups (proprietary, lightweight and large-scale open-source) show similar performance, each achieving an MF1 score above 0.75. For the counting request, *Gemini 2.5 Pro* clearly leads with a substantial margin, even over other proprietary models such as *o1* and *o3*. However, as shown in Figure 8 (Appendix A), even the best-performing models tend to produce accurate counts primarily when the ground-truth is 1 or 2, but exhibit a tendency to undercount as the true value increases. Finally, for name-listing, *Qwen-VL 2.5 7B/72B* and *Gemini 2.5 Pro* deliver similar highest performance among all evaluated models.

Multiple-Type Map Feature (MTMF): This task asked two requests simultaneously: counting and name-listing. To assess overall performance, we calculate metrics separately for all MF types within each CM, and then average them across all CMs. Therefore, for counting, we report the average RMSE (aRMSE) and average r^2 (ar^2); while for name-listing, we use average of micro precision (amPrec.), average of micro recall (amRec.), and average of micro F1-score (amF1).

As shown in Table 5, all LLMs outperform the *Random* baseline. Among them, *o1* ranks higher across most metrics, followed by *o3* and *Gemini 2.5 Pro*. Despite this, the overall low scores of all models

indicate that LVLMS struggle with this more complex, multi-type reasoning task. Additional comparisons in Table 10 (Appendix A) show that performance on MTMF is consistently lower than on the STMF task, on both requests and across most models, confirming that handling multiple MFs simultaneously is more challenging than addressing them individually.

Map Marker Localization (MML): Table 6 reports models overall accuracy on this task, along with breakdowns by marker color and zoom-in level. *Gemini 2.5 Pro* again exhibits superior performance with a large margin over all other models. Among open-source options, *Qwen-VL 2.5 7B* and *72B* achieve the highest accuracy in the lightweight and large-scale groups, respectively. Performance is consistent across marker colors, suggesting that color variation does not significantly impact model detection ability. However, accuracy increases with higher zoom-in level (i.e., more focused views), suggesting that reduced information facilitates marker detection. Despite these trends, all models still exhibit relatively low overall accuracy, underscoring the crucial need for improvements before addressing more demanding tasks that rely on accurate marker localization—such as the SRN task.

Route Length Estimation (RLE): This task requires LVLMS to perform multiple intermediate reasoning steps, ultimately estimating real-world distances. Note that each request specified the unit for length measurement: either meters or feet. To support this process, we employed a chain-of-thought (CoT) [49] prompting strategy, guiding models through step-by-step reasoning for route length estimation. Due to space constraints, the detailed CoT prompt is available in our source code. Table 11 (Appendix A) demonstrates that such an enhancement improves performance across most models and metrics compared to a non-CoT strategy.

Table 7 lists the complete results of this task using the CoT prompt, with *o1* and *o3* achieving the top two scores across most cases and metrics. For open-source models, *Qwen-VL 2.5 72B* delivered the best results, but it frequently repeats specific numbers regardless of the provided CM (as illustrated in Figure 10b from Appendix A). This behavior likely stems from its difficulty in detecting map markers (as evidenced in Table 6), leading to failures in identifying the blue path and, consequently, generating arbitrary length estimates. Despite improvements with CoT prompting, error rates remain high across all models, especially open-source ones. Such an observation further highlights the challenge associated to these tasks and the need for further advancement.

Shortest Route Navigation (SRN): Evaluation results for this task are presented in Table 8. It includes both the overall scores and breakdowns by zoom-in level. As with previous tasks, proprietary models outperform open-source ones, with *o3* achieving the highest overall performance, followed by *o1*. However, *o3* performance remains modest with only 33.8% of proposed routes matching the shortest routes (SR^2) and 37.8% of the routes that correctly connect both starting and destination markers (connectivity). Open-source models perform significantly worse, with their generated routes rarely matching the true shortest path. While inaccurate marker localization is likely a contributing factor, this does not fully explain the poor performance. In fact, *Gemini 2.5 Pro*, which achieves the highest accuracy (0.6) in the MML task, only attains low SR^2 (0.184) and connectivity (0.273) scores. This suggests that other factors, such as limited geospatial reasoning abilities, may also be at play.

Table 6: Main results of the Map Marker Localization (MML) task. Bold and underlined values indicate the best and second-best performance, respectively, within each group of models.

Model	Acc. (↑)					
	Marker color		Zoom-in level			Overall
	Blue	Red	17	18	19	
LLama 3.2 11B	<u>0.128</u>	<u>0.128</u>	0.106	0.038	<u>0.263</u>	<u>0.128</u>
InternVL 2.5 8B	0.112	0.056	0.000	0.029	0.225	0.084
LLaVa-OV 7B	0.048	0.048	0.000	0.019	0.125	0.048
Qwen-VL 2.5 7B	0.248	0.240	<u>0.096</u>	0.152	0.513	0.244
LLama 4 Scout	<u>0.260</u>	<u>0.264</u>	0.029	0.333	<u>0.500</u>	<u>0.260</u>
LLama 3.2 90B	0.136	0.152	0.038	0.091	0.325	0.144
InternVL 2.5 78B	0.112	0.176	<u>0.048</u>	0.106	0.300	0.144
LLaVa-OV 72B	0.080	0.088	0.000	0.091	0.188	0.084
Qwen-VL 2.5 72B	0.288	0.304	0.197	<u>0.173</u>	0.538	0.296
GPT-4(V)	0.064	0.096	0.077	0.030	0.125	0.080
GPT-4o	0.344	0.360	0.240	0.242	0.588	0.352
o1	<u>0.416</u>	<u>0.432</u>	<u>0.308</u>	<u>0.379</u>	<u>0.613</u>	<u>0.424</u>
o3	0.304	0.304	0.212	0.227	<u>0.613</u>	0.344
Gemini 2.5 Pro	0.608	0.592	0.471	0.636	0.738	0.600
Claude 3.7 Sonnet	0.224	0.240	0.135	0.227	0.363	0.232

As observed in the MML, performance improves with higher zoom-in level, one more time suggesting that more focused map views—with reduced contextual information—facilitate tasks resolution. Altogether, these findings again highlight a substantial gap in current LVLMS capabilities to perform this task accordingly and more generally complex geospatial reasoning. They also emphasize the need to expand Car to MapQA in the future with additional tasks to better uncover and address the root causes of these limitations.

4.4 Analysis and discussions

This section provides a deeper analysis of LVLMS’ performance across all objectives and discusses key insights and potential directions for enhancing their understanding of CM.

Map Feature Understanding: We examined 50% of incorrect answers on the name-listing request in the STMF task, from *Qwen-VL 2.5 72B* and *Gemini 2.5 Pro*—the top-performing open-source and proprietary models, respectively. Such an analysis revealed three main issues: object hallucination, incorrect association of MF type (misrecognition), and OCR errors. Figure 4 provides examples of each issue and their occurrence across both models. Hallucination was rare, with only one or two occurrences per model, indicating that both models generally base their answers on visible content in the CM. However, misrecognition and OCR errors were far more prevalent. In the case of misrecognition, while LVLMS can detect POI and read associated names on CMs, they often struggle to assign them to the correct MF types—frequently confusing closely related types such as restaurants, fast-food stores, and coffee shops (see Figure 11 from Appendix A).

These findings highlight two critical limitations: (1) current OCR capabilities are not sufficiently robust for cartographic tasks, and (2) semantic reasoning for visual entities remains shallow, particularly when distinguishing between conceptually adjacent types. A promising direction for future work is to enhance the vision encoder, such as using a high-resolution or map-specific encoder.

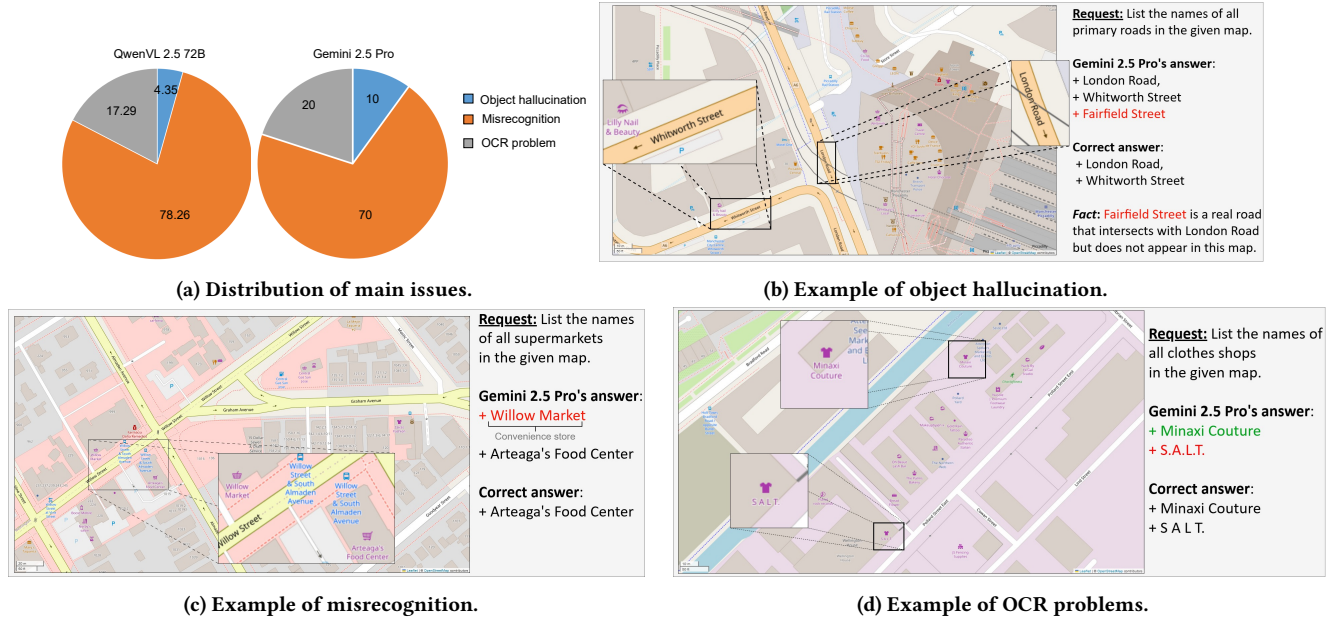


Figure 4: Distribution and examples of the main issues identified in 50% of the incorrect answers from *Gemini 2.5 Pro* and *Qwen-VL 2.5 72B* in the Single-Type Map Feature (STMF) task with name-listing requests. Note: due space constraints, requests shown are short versions of the actual ones.

Map Scale Understanding: We analyzed 50 randomly selected responses from *o1* on the RLE task, which demonstrated the highest performances across most cases and metrics. This review revealed one key strength: the model demonstrates a solid ability to read the scale bar, accurately extracting its numerical value and associated unit, in 84% of cases. An illustrative example is shown in Figure 9 from Appendix A. However, this analysis also unveiled an unexpected behavior: in 8% of these responses, the model attempted to interpret the scale unit into inches or centimeters—units irrelevant to the context of CMs. This suggests occasional confusion possibly stemming from the data used during training.

While *o1* shows promising capabilities, its non-negligible error rate demonstrate that models could be improved. Future work could investigate specialized pretraining or alignment strategies to better capture scale, numeric value and unit as well as estimate distance.

Map Navigation: We analyzed 30% of incorrect routes (randomly selected) provided by the *o3* model—the top performer on this task—to understand the sources of failure. Figure 5a presents the distribution of six most frequent error types observed: (i) Incorrect name of the road associated to the origin or destination (22%): These issues could stem from inaccurate localization of map markers or misidentification of road names. (ii) Incorrect direction changes (18%): The model frequently failed to accurately provide

Table 7: Main results of the Route Length Estimation (RLE) task. Bold and underlined values indicate the best and second-best performance, respectively, within each group of models.

Model	Simple						Complex					
	Meter			Feet			Meter			Feet		
	RMSE (↓)	MAPE (↓)	r^2 (↑)	RMSE (↓)	MAPE (↓)	r^2 (↑)	RMSE (↓)	MAPE (↓)	r^2 (↑)	RMSE (↓)	MAPE (↓)	r^2 (↑)
LLama 3.2 11B	1446.46	16.80	-44.91	1474.81	4.83	-3.43	1651.13	4.91	-6.88	2023.44	1.02	-0.10
InternVL 2.5 8B	601.30	7.66	-6.93	1416.15	2.85	-3.09	804.98	2.15	-0.87	2125.96	0.91	-0.21
LLaVa-OV 7B	586.83	11.79	-6.56	711.12	3.10	-0.03	600.19	2.21	-0.04	2288.64	0.76	-0.41
Qwen-VL 2.5 7B	543.59	4.29	-5.48	714.44	2.26	-0.04	647.80	2.05	-0.21	1852.24	0.97	0.08
LLama 4 Scout	250.32	1.44	-0.37	1837.56	1.34	-5.88	518.02	0.67	0.22	2251.80	0.72	-0.36
LLama 3.2 90B	318.40	5.48	-1.22	655.49	2.81	0.12	562.66	1.26	0.08	1499.69	0.63	0.40
InternVL 2.5 78B	363.22	3.55	-1.89	618.14	1.44	0.22	509.27	1.06	0.25	1911.23	0.61	0.02
LlaVa-OV 72B	530.95	3.62	-5.19	671.92	1.84	0.08	626.88	1.71	-0.14	1978.15	0.64	-0.05
Qwen-VL 2.5 72B	170.43	1.31	0.36	471.57	0.58	0.55	433.74	0.46	0.46	1914.02	0.50	0.02
GPT-4(V)	271.15	0.97	-0.61	549.96	0.86	0.38	449.77	0.48	0.42	1678.36	0.53	0.24
GPT-4o	208.86	0.93	0.04	526.32	0.51	0.44	314.93	0.42	0.71	1344.83	0.42	0.51
o1	104.25	0.52	0.76	290.88	0.43	0.83	305.12	0.32	0.73	1096.74	0.40	0.68
o3	91.69	0.70	0.82	476.21	0.55	0.54	386.96	0.33	0.57	1519.38	0.36	0.38
Gemini 2.5 Pro	127.25	0.53	0.64	485.77	0.42	0.52	458.06	0.43	0.39	1856.34	0.55	0.07
Claude 3.7 Sonnet	130.64	0.82	0.63	506.15	0.44	0.48	454.79	0.44	0.40	1899.86	0.55	0.03

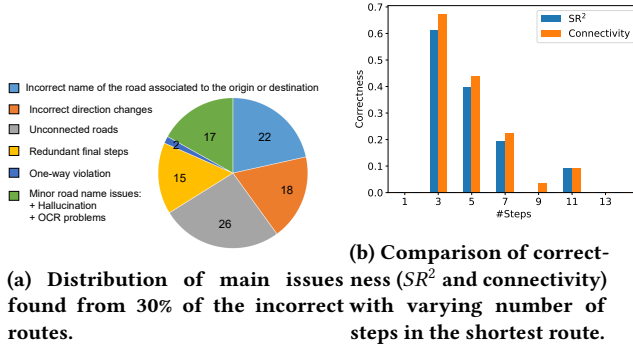


Figure 5: Analysis from the $o3$ model in the Shortest Route Navigation (SRN) task.

turning directions, likely reflecting limitations in geospatial reasoning or misinterpretation of road layouts. (iii) Unconnected roads (26%): The most prevalent issue, where the model suggested paths that involve transitions between roads that are not physically connected, indicating gaps in topological map understanding. (iv) One-way violations (2%): Although rare, these errors—where the model proposed driving against one-way traffic—are critical. They may result from an inability to detect one-way indicators (e.g., arrows), and pose significant safety risks in real-world navigation tasks. (v) Redundant final steps (15%): The model occasionally added additional steps after reaching the destination, causing unnecessary detours. This suggests a lack of clear identification of the destination or routing capabilities. (vi) Minor road name issues (17%): These include hallucinated or incorrectly read road names, again demonstrating OCR limitations. Figure 12 and 13 in Appendix A illustrate examples of these failure types and of correctly generated routes, respectively.

To further assess model performance, Figure 5b examines $o3$ scores based on the number of steps in the shortest route. Notably, the model achieves SR^2 scores over 0.4 for short routes requiring only three to five steps (i.e., one or two turns), but performance rapidly declines for longer, more complex routes, highlighting a key limitation. These findings underscore that while $o3$ exhibits

some geospatial reasoning capabilities, it might lack robust topological awareness, road segmentation capability and context-sensitive route planning. Future research might explore hybrid approaches combining LVLMs with graph-based map parsers, or strategies to gradually build up complex navigation skills.

5 Conclusion and future work

In this paper, we introduced CartoMapQA, a benchmark dataset designed to assess the capabilities of Large Visual-Language Models (LVLMs) in understanding cartographic map. CartoMapQA tests a broad range of skills—i.e., map features, and their associated text, recognition and extraction, scale interpretation, directional understanding, and turn-by-turn navigation—essential for comprehensive Cartographic Map (CM) comprehension and geospatial reasoning. Our evaluations reveal that, despite recent progress, current LVLMs still face significant challenges in reasoning over CMs, particularly in handling complex geospatial tasks. By structuring CartoMapQA into a hierarchy of tasks with increasing complexity, we provide a rigorous and valuable benchmark that not only help identifying specific weaknesses but also supports the development of more robust, map-aware LVLMs.

The insights gained from our study can inform future efforts on how to fine-tune or design LVLm architectures tailored to the challenges of cartographic reasoning. Future directions include expanding CartoMapQA with additional tasks to expose more nuanced limitations, and exploring advanced capabilities such as complex navigation and social indicator estimation.

References

- [1] Josh Achiam, Steven Adler, Sandhini Agarwal, Lama Ahmad, Ilge Akkaya, Florencia Leoni Aleman, Diogo Almeida, Janko Altschmidt, Sam Altman, Shyamal Anadkat, et al. 2024. Gpt-4 technical report. arXiv:2303.08774 [cs.CL] <https://arxiv.org/abs/2303.08774>
- [2] Janice Ahn, Rishu Verma, Renze Lou, Di Liu, Rui Zhang, and Wenpeng Yin. 2024. Large Language Models for Mathematical Reasoning: Progresses and Challenges. arXiv:2402.00157 [cs.CL] <https://arxiv.org/abs/2402.00157>
- [3] Jean-Baptiste Alayrac, Jeff Donahue, Pauline Luc, Antoine Miech, Iain Barr, Yana Hasson, Karel Lenc, Arthur Mensch, Katherine Millican, Malcolm Reynolds, et al. 2022. Flamingo: a visual language model for few-shot learning. *Advances in neural information processing systems* 35 (2022), 23716–23736.
- [4] Anthropic. 2025. Claude 3.7 Sonnet. <https://www.anthropic.com/claude/sonnet>
- [5] Jinze Bai, Shuai Bai, Shusheng Yang, Shijie Wang, Sinan Tan, Peng Wang, Junyang Lin, Chang Zhou, and Jingren Zhou. 2023. Qwen-vl: A frontier large vision-language model with versatile abilities. arXiv:2308.12966 [cs.CV] <https://arxiv.org/abs/2308.12966>

Table 8: Main results of the Shortest Route Navigation (SRN) task. Bold and underlined values indicate the best and second-best performance, respectively, within each group of models.

Model	Zoom-in level									Overall		
	Zoom 17			Zoom 18			Zoom 19			SR ² (↑)	aSA(↑)	Connectivity (↑)
LLama 3.2 11B	0.000	0.047	0.000	0.000	0.078	0.011	0.000	0.111	0.024	0.000	0.077	0.011
InternVL 2.5 8B	0.000	0.030	0.000	0.000	0.059	0.000	0.000	0.046	0.012	0.000	0.045	0.004
LLaVa-OV 7B	0.000	0.071	0.000	0.000	0.062	0.000	0.000	0.038	0.012	0.000	0.058	0.004
Qwen-VL 2.5 7B	0.000	0.094	0.000	0.000	0.126	0.000	0.000	0.086	0.000	0.000	0.102	0.000
LLama 4 Scout	0.000	0.028	0.000	0.000	0.122	0.011	0.024	0.119	0.024	0.007	0.086	0.011
LLama 3.2 90B	0.000	0.096	0.000	0.000	0.151	0.011	0.000	0.115	0.012	0.000	0.119	0.007
InternVL 2.5 78B	0.000	0.064	0.000	0.000	0.097	0.000	0.000	0.105	0.024	0.000	0.087	0.007
LLaVa-OV 72B	0.010	0.087	0.010	0.011	0.172	0.034	0.000	0.154	0.012	0.007	0.135	0.018
Qwen-VL 2.5 72B	0.000	0.099	0.010	0.000	0.228	0.022	0.036	0.205	0.060	0.011	0.173	0.029
GPT-4(V)	0.000	0.023	0.029	0.000	0.069	0.045	0.024	0.082	0.107	0.007	0.056	0.058
GPT-4o	0.010	0.084	0.019	0.022	0.135	0.101	0.060	0.184	0.107	0.029	0.131	0.072
o1	0.133	0.278	0.200	0.281	0.419	0.404	0.464	0.419	0.500	0.281	0.423	0.356
o3	0.238	0.352	0.267	0.292	0.448	0.326	0.512	0.665	0.571	0.338	0.477	0.378
Gemini 2.5 Pro	0.067	0.167	0.124	0.157	0.307	0.258	0.357	0.307	0.476	0.184	0.311	0.273
Claude 3.7 Sonnet	0.105	0.188	0.124	0.101	0.209	0.191	0.155	0.241	0.238	0.119	0.211	0.180

- org/abs/2308.12966
- [6] Shuai Bai, Keqin Chen, Xuejing Liu, Jialin Wang, Wenbin Ge, Sibo Song, Kai Dang, Peng Wang, Shijie Wang, Jun Tang, Humen Zhong, Yuanzhi Zhu, Mingkun Yang, Zhaohai Li, Jianqiang Wan, Pengfei Wang, Wei Ding, Zheren Fu, Yiheng Xu, Jiabo Ye, Xi Zhang, Tianbao Xie, Zesen Cheng, Hang Zhang, Zhibo Yang, Haiyang Xu, and Junyang Lin. 2025. Qwen2.5-VL Technical Report. arXiv:2502.13923 [cs.CV] <https://arxiv.org/abs/2502.13923>
- [7] Prabin Bhandari, Antonios Anastasopoulos, and Dieter Pfoser. 2023. Are large language models geospatially knowledgeable?. In *Proceedings of the 31st ACM International Conference on Advances in Geographic Information Systems*. ACM, NY, US, 1–4.
- [8] Geoff Boeing. 2025. Modeling and Analyzing Urban Networks and Amenities with OSMnx. arXiv:2505.00736 [physics.soc-ph] <https://arxiv.org/abs/2505.00736>
- [9] Zhe Chen, Weiyun Wang, Yue Cao, Yangzhou Liu, Zhangwei Gao, Erfei Cui, Jinguo Zhu, Shenglong Ye, Hao Tian, Zhaoyang Liu, et al. 2025. Expanding Performance Boundaries of Open-Source Multimodal Models with Model, Data, and Test-Time Scaling. arXiv:2412.05271 [cs.CV] <https://arxiv.org/abs/2412.05271>
- [10] Zhe Chen, Weiyun Wang, Hao Tian, Shenglong Ye, Zhangwei Gao, Erfei Cui, Wenwen Tong, Kongzhi Hu, Jiapeng Luo, Zheng Ma, et al. 2024. How far are we to gpt-4v? closing the gap to commercial multimodal models with open-source suites. arXiv:2404.16821 [cs.CV] <https://arxiv.org/abs/2404.16821>
- [11] Zhe Chen, Jiannan Wu, Wenhai Wang, Weijie Su, Guo Chen, Sen Xing, Muyan Zhong, Qinglong Zhang, Xizhou Zhu, Lewei Lu, Bin Li, Ping Luo, Tong Lu, Yu Qiao, and Jifeng Dai. 2024. InternVL: Scaling up Vision Foundation Models and Aligning for Generic Visual-Linguistic Tasks. arXiv:2312.14238 [cs.CV] <https://arxiv.org/abs/2312.14238>
- [12] Anthony G Cohn and Robert E Blackwell. 2024. Evaluating the Ability of Large Language Models to Reason About Cardinal Directions. In *16th International Conference on Spatial Information Theory (COSIT 2024)*. Schloss Dagstuhl–Leibniz-Zentrum für Informatik, Quebec, Canada.
- [13] Google DeepMind. 2025. Gemini 2.5: Our most intelligent AI model. <https://blog.google/technology/google-deepmind/gemini-model-thinking-updates-march-2025/#gemini-2-5-thinking>
- [14] Cheng Deng, Tianhang Zhang, Zhongmou He, Qiyuan Chen, Yuanyuan Shi, Yi Xu, Luoyi Fu, Weinan Zhang, Xinbing Wang, Chenghu Zhou, et al. 2024. K2: A foundation language model for geoscience knowledge understanding and utilization. In *Proceedings of the 17th ACM International Conference on Web Search and Data Mining*. ACM, NY, US, 161–170.
- [15] Mahir Labib Dihan, Md Tanvir Hassan, Md Tanvir Parvez, Md Hasebul Hasan, Md Almash Alam, Muhammad Aamir Cheema, Mohammed Eunus Ali, and Md Rizwan Parvez. 2025. MapEval: A Map-Based Evaluation of Geo-Spatial Reasoning in Foundation Models. In *International Conference on Machine Learning*. PMLR, Vancouver, Canada, 13774–13813.
- [16] Abhimanyu Dubey, Abhinav Jauhri, Abhinav Pandey, Abhishek Kadian, Ahmad Al-Dahle, Aiesha Letman, Akhil Mathur, Alan Schelten, Amy Yang, Angela Fan, et al. 2024. The llama 3 herd of models. arXiv:2407.21783 [cs.AI] <https://arxiv.org/abs/2407.21783>
- [17] Jie Feng, Jun Zhang, Junbo Yan, Xin Zhang, Tianjian Ouyang, Tianhui Liu, Yuwei Du, Siqi Guo, and Yong Li. 2025. CityBench: Evaluating the Capabilities of Large Language Model as World Model. arXiv:2406.13945 [cs.AI] <https://arxiv.org/abs/2406.13945>
- [18] Peng Gao, Jiaming Han, Renrui Zhang, Ziyi Lin, Shijie Geng, Aojun Zhou, Wei Zhang, Pan Lu, Conghui He, Xiangyu Yue, et al. 2023. Llama-adapter v2: Parameter-efficient visual instruction model. arXiv:2304.15010 [cs.CV] <https://arxiv.org/abs/2304.15010>
- [19] Aaron Grattafiori, Abhimanyu Dubey, Abhinav Jauhri, Abhinav Pandey, Abhishek Kadian, Ahmad Al-Dahle, Aiesha Letman, Akhil Mathur, Alan Schelten, Alex Vaughan, et al. 2024. The llama 3 herd of models. arXiv:2407.21783 [cs.AI] <https://arxiv.org/abs/2407.21783>
- [20] Wes Gurnee and Max Tegmark. 2024. Language Models Represent Space and Time. In *The Twelfth International Conference on Learning Representations*. ICLR, Vienna, Austria, 1–21.
- [21] Aric Hagberg, Pieter J Swart, and Daniel A Schult. 2008. *Exploring network structure, dynamics, and function using NetworkX*. Technical Report. Los Alamos National Laboratory (LANL), Los Alamos, NM (United States).
- [22] Sirui Hong, Mingchen Zhuge, Jonathan Chen, Xianwu Zheng, Yuheng Cheng, Jinlin Wang, Ceyao Zhang, Zili Wang, Steven Ka Shing Yau, Zijuan Lin, et al. 2024. MetaGPT: Meta Programming for A Multi-Agent Collaborative Framework. In *The Twelfth International Conference on Learning Representations*. ICLR, Vienna, Austria, 1–29.
- [23] Wenyi Hong, Weihang Wang, Ming Ding, Wenmeng Yu, Qingsong Lv, Yan Wang, Yeon Cheng, Shiyu Huang, Junhui Ji, Zhao Xue, et al. 2024. CogVLM2: Visual language models for image and video understanding. arXiv:2408.16500 [cs.CV] <https://arxiv.org/abs/2408.16500>
- [24] Aaron Hurst, Adam Lerer, Adam P Goucher, Adam Perelman, Aditya Ramesh, Aidan Clark, AJ Ostrow, Akila Welihinda, Alan Hayes, Alec Radford, et al. 2024. Gpt-4o system card. arXiv:2410.21276 [cs.CL] <https://arxiv.org/abs/2410.21276>
- [25] Aaron Jaech, Adam Kalai, Adam Lerer, Adam Richardson, Ahmed El-Kishky, Aiden Low, Alec Helyar, Aleksander Madry, Alex Beutel, Alex Carney, et al. 2024. Openai o1 system card. arXiv:2412.16720 [cs.AI] <https://arxiv.org/abs/2412.16720>
- [26] Kartik Kuckreja, Muhammad Sohail Danish, Muzammal Naseer, Abhijit Das, Salman Khan, and Fahad Shahbaz Khan. 2024. Geochat: Grounded large vision-language model for remote sensing. In *Proceedings of the IEEE/CVF Conference on Computer Vision and Pattern Recognition*. IEEE Computer Society, Seattle WA, US, 27831–27840.
- [27] Bo Li, Kaichen Zhang, Hao Zhang, Dong Guo, Renrui Zhang, Feng Li, Yuanhan Zhang, Ziwei Liu, and Chunyuan Li. 2024. LLaVA-NeXT: Stronger LLMs Supercharge Multimodal Capabilities in the Wild. <https://llava-vl.github.io/blog/2024-05-10-llava-next-stronger-llms/>
- [28] Bo Li, Yuanhan Zhang, Dong Guo, Renrui Zhang, Feng Li, Hao Zhang, Kaichen Zhang, Yanwei Li, Ziwei Liu, and Chunyuan Li. 2024. LLaVA-OneVision: Easy Visual Task Transfer. arXiv:2408.03326 [cs.CV] <https://arxiv.org/abs/2408.03326>
- [29] Ji Lin, Hongxu Yin, Wei Ping, Pavlo Molchanov, Mohammad Shoeybi, and Song Han. 2024. Vila: On pre-training for visual language models. In *Proceedings of the IEEE/CVF Conference on Computer Vision and Pattern Recognition*. IEEE Computer Society, Seattle WA, US, 26689–26699.
- [30] Haotian Liu, Chunyuan Li, Yuheng Li, and Yong Jae Lee. 2024. Improved baselines with visual instruction tuning. In *Proceedings of the IEEE/CVF Conference on Computer Vision and Pattern Recognition*. IEEE Computer Society, Seattle WA, US, 26296–26306.
- [31] Haotian Liu, Chunyuan Li, Qingyang Wu, and Yong Jae Lee. 2023. Visual instruction tuning. *Advances in neural information processing systems* 36 (2023), 34892–34916.
- [32] Sylvain Lobry, Diego Marcos, Jesse Murray, and Devis Tuia. 2020. RSVQA: Visual question answering for remote sensing data. *IEEE Transactions on Geoscience and Remote Sensing* 58, 12 (2020), 8555–8566.
- [33] Rohin Manvi, Samar Khanna, Gengchen Mai, Marshall Burke, David B Lobell, and Stefano Ermon. 2024. GeoLLM: Extracting Geospatial Knowledge from Large Language Models. In *The Twelfth International Conference on Learning Representations*. ICLR, Vienna, Austria, 1–17.
- [34] Meta. 2024. Llama-3.2-11b-vision-instruct. <https://huggingface.co/meta-llama/Llama-3.2-11B-Vision-Instruct>
- [35] Meta. 2024. Llama-3.2-90b-vision-instruct. <https://huggingface.co/meta-llama/Llama-3.2-90B-Vision-Instruct>
- [36] Meta. 2025. Llama-4-Scout-17B-16E-Instruct. <https://huggingface.co/meta-llama/Llama-4-Scout-17B-16E-Instruct>
- [37] Peter Mooney, Wencong Cui, Boyuan Guan, and Levente Juhász. 2023. Towards understanding the geospatial skills of chatgpt: Taking a geographic information systems (gis) exam. In *Proceedings of the 6th ACM SIGSPATIAL International Workshop on AI for Geographic Knowledge Discovery*. ACM, Hamburg, Germany, 85–94.
- [38] OpenAI. 2022. Introducing ChatGPT. <https://openai.com/blog/chatgpt>
- [39] OpenAI. 2025. OpenAI o3 and o4-mini System Card. <https://cdn.openai.com/pdf/2221c875-02dc-4789-800b-e7758f3722c1/o3-and-o4-mini-system-card.pdf>
- [40] OpenStreetMap contributors. 2017. Planet dump retrieved from <https://planet.osm.org>. <https://www.openstreetmap.org>
- [41] Zhiliang Peng, Wenhui Wang, Li Dong, Yaru Hao, Shaohan Huang, Shuming Ma, and Furu Wei. 2023. Kosmos-2: Grounding multimodal large language models to the world. arXiv:2306.14824 [cs.CL] <https://arxiv.org/abs/2306.14824>
- [42] python visualization. 2020. *Folium*. <https://python-visualization.github.io/folium/>
- [43] Alec Radford, Jong Wook Kim, Chris Hallacy, Aditya Ramesh, Gabriel Goh, Sandhini Agarwal, Girish Sastry, Amanda Askell, Pamela Mishkin, Jack Clark, et al. 2021. Learning transferable visual models from natural language supervision. In *International conference on machine learning*. PMLR, Virtual conference, 8748–8763.
- [44] Jonathan Roberts, Timo Lüddecke, Sowmen Das, Kai Han, and Samuel Al-banie. 2023. GPT4GEO: How a Language Model Sees the World’s Geography. arXiv:2306.00020 [cs.CL] <https://arxiv.org/abs/2306.00020>
- [45] Mirac Suzgun, Nathan Scales, Nathanael Schärli, Sebastian Gehrmann, Yi Tay, Hyung Won Chung, Aakanksha Chowdhery, Quoc Le, Ed Chi, Denny Zhou, et al. 2023. Challenging BIG-Bench Tasks and Whether Chain-of-Thought Can Solve Them. In *Findings of the Association for Computational Linguistics: ACL 2023*. ACL Anthology, Toronto, Canada, 13003–13051.
- [46] Zhiheng Tang and Mayank Kejriwal. 2025. GRASP: A Grid-Based Benchmark for Evaluating Commonsense Spatial Reasoning. arXiv:2407.01892 [cs.AI] <https://arxiv.org/abs/2407.01892>
- [47] Wenhai Wang, Zhe Chen, Xiaokang Chen, Jiannan Wu, Xizhou Zhu, Gang Zeng, Ping Luo, Tong Lu, Jie Zhou, Yu Qiao, and Jifeng Dai. 2023. VisionLLM: Large Language Model is also an Open-Ended Decoder for Vision-Centric Tasks. In *Advances in Neural Information Processing Systems*, Vol. 36. Curran Associates, Inc., New Orleans, US, 61501–61513.
- [48] Weihang Wang, Qingsong Lv, Wenmeng Yu, Wenyi Hong, Ji Qi, Yan Wang, Junhui Ji, Zhuoyi Yang, Lei Zhao, Xixuan Song, Jiazheng Xu, Keqin Chen, Bin Xu, Juanzi Li, Yuxiao Dong, Ming Ding, and Jie Tang. 2024. CogVLM: Visual Expert

- for Pretrained Language Models. In *Advances in Neural Information Processing Systems*, Vol. 37. Curran Associates, Inc., Vancouver, Canada, 121475–121499.
- [49] Jason Wei, Xuezhi Wang, Dale Schuurmans, Maarten Bosma, Fei Xia, Ed Chi, Quoc V Le, Denny Zhou, et al. 2022. Chain-of-thought prompting elicits reasoning in large language models. *Advances in neural information processing systems* 35 (2022), 24824–24837.
 - [50] Runsen Xu, Wei Yao Wang, Hao Tang, Xingyu Chen, Xiaodong Wang, Fu-Jen Chu, Dahua Lin, Matt Feiszli, and Kevin J Liang. 2025. Multi-SpatialMLLM: Multi-Frame Spatial Understanding with Multi-Modal Large Language Models. arXiv:2505.17015 [cs.CV] <https://arxiv.org/abs/2505.17015>
 - [51] Yutaro Yamada, Yihan Bao, Andrew K. Lampinen, Jungo Kasai, and Ilker Yildirim. 2024. Evaluating Spatial Understanding of Large Language Models. arXiv:2310.14540 [cs.CL] <https://arxiv.org/abs/2310.14540>
 - [52] Yibo Yan, Haomin Wen, Siru Zhong, Wei Chen, Haodong Chen, Qingsong Wen, Roger Zimmermann, and Yuxuan Liang. 2024. Urbanclip: Learning text-enhanced urban region profiling with contrastive language-image pretraining from the web. In *Proceedings of the ACM on Web Conference 2024*. ACM, NY, US, 4006–4017.
 - [53] Jihan Yang, Runyu Ding, Ellis Brown, Xiaojuan Qi, and Saining Xie. 2024. V-IRL: Grounding Virtual Intelligence in Real Life. arXiv:2402.03310 [cs.AI] <https://arxiv.org/abs/2402.03310>
 - [54] Xiang Yue, Yuansheng Ni, Kai Zhang, Tianyu Zheng, Ruoqi Liu, Ge Zhang, Samuel Stevens, Dongfu Jiang, Weiming Ren, Yuxuan Sun, et al. 2024. Mmmu: A massive multi-discipline multimodal understanding and reasoning benchmark for expert agi. In *Proceedings of the IEEE/CVF Conference on Computer Vision and Pattern Recognition*. IEEE Computer Society, Seattle WA, US, 9556–9567.
 - [55] Chenhui Zhang and Sherrie Wang. 2024. Good at captioning, bad at counting: Benchmarking gpt-4v on earth observation data. In *Proceedings of the IEEE/CVF Conference on Computer Vision and Pattern Recognition Workshops*. IEEE Computer Society, Seattle WA, US, 7839–7849.
 - [56] Deyao Zhu, Jun Chen, Xiaoqian Shen, Xiang Li, and Mohamed Elhoseiny. 2024. MiniGPT-4: Enhancing Vision-Language Understanding with Advanced Large Language Models. In *The Twelfth International Conference on Learning Representations*. ICLR, Vienna, Austria, 1–17.

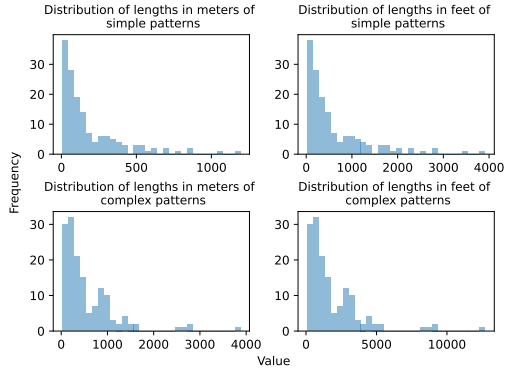


Figure 6: Distribution of route lengths in the Route Length Estimation (RLE) task.

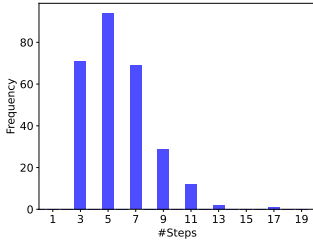


Figure 7: Distribution of the number of steps in the Shortest Route Navigation (SRN) task.

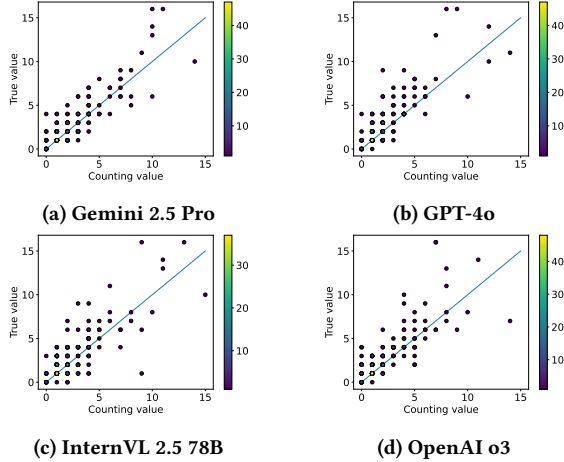


Figure 8: Scatter plots of true versus counts estimated by LVLs. Blue lines indicate correct estimation. To address overlapping points with identical true and estimated values, color gradients represent point density for improved visual clarity.

Table 11: Comparison on the performance with (w/) and without (w/o) the chain-of-thought (CoT) strategy. Experiments were performed with two advanced proprietary models that lack native extended thinking ability.

	Simple				Complex			
	Meter		Feet		Meter		Feet	
	RMSE (↓)	r^2 (↑)	RMSE (↓)	r^2 (↑)	RMSE (↓)	r^2 (↑)	RMSE (↓)	r^2 (↑)
GPT-4(V) w/o CoT	146.79	0.53	638.93	0.17	468.02	0.37	2040.8	-0.11
GPT-4(V) w/ CoT	271.15	-0.61	549.96	0.38	449.77	0.42	1678.36	0.24
GPT-4o w/o CoT	249.73	-0.37	966.10	-0.9	534.51	0.17	1733.21	0.19
GPT-4o w/ CoT	208.86	0.04	526.32	0.44	314.93	0.71	1344.83	0.51

Table 9: Description of map features utilized in the Single-Type Map Feature (STMF) and the Multiple-Type Map Feature (MTMF) tasks.

No.	Type	Category	Class	Image
1	Convenience store	Symbol	Shop	
2	Supermarket	Symbol	Shop	
3	Drug store/pharmacy	Symbol	Amenity	
4	General clinic	Symbol	Amenity	
5	Hospital	Symbol	Amenity	
6	Restaurant	Symbol	Amenity	
7	Fast food store	Symbol	Amenity	
8	Coffee shop	Symbol	Amenity	
9	ATM or cash point	Symbol	Amenity	
10	Bank	Symbol	Amenity	
11	Playground	Symbol	Leisure	
12	Park area	Area	Leisure	
13	Fitness center	Symbol	Leisure	
14	Clothes shop	Symbol	Shop	
15	Beauty shop	Symbol	Shop	
16	Water stream	Line	Waterway	
17	River	Line	Waterway	
18	Bus stop	Symbol	Highway	
19	Gas station	Symbol	Amenity	
20	Primary road	Line	Highway	
21	Car parking lot	Symbol	Amenity	
22	Public toilet	Symbol	Amenity	

A Appendix

The list of MFs is provided in Table 9. Figure 6 and 7 show the distribution plots described in Section 3.1 for MTMF and SRN, respectively. Figure 8 illustrates the models' tendency to undercount. Table 10 further compares STMF and MTMF results, as discussed in Section 4.3, while Table 11 reports results with and without CoT. Figure 11 presents a confusion matrix highlighting potential misrecognition or OCR errors. Figure 10 compares real and estimated lengths across models as mentioned in Section 4.3. Figure 9 presents an example of correctly interpreting the scale bar. Finally, Figure 12 and 13 illustrate representative failure cases and correctly generated routes, respectively.

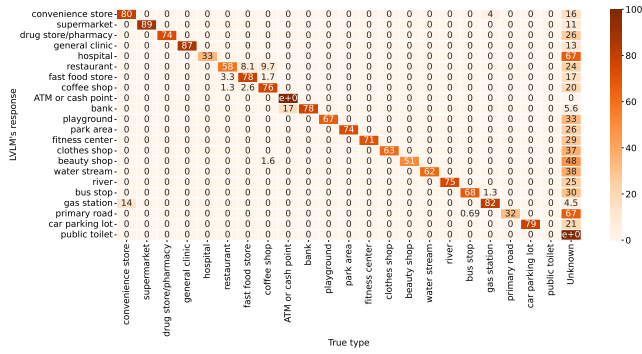


Figure 11: Confusion matrix of OpenAI o1's responses to the name-listing request in the Multiple-Type Map Feature (MTMF) task. Each cell represents a percentage, where the values of each row sum to 100%. The final column, "Unknown", corresponds to names that do match any of the considered MF types, and may potentially result from OCR errors or hallucinations.

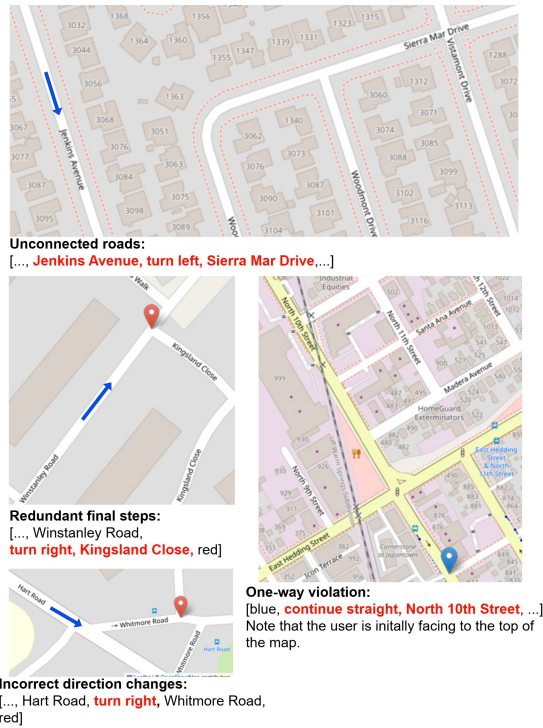


Figure 12: Examples of issues found in o3's responses in the Shortest Route Navigation (SRN) task. Notes: due to space constraints, the Cartographic Maps are cropped from the original inputs. And, blue arrows are overlaid to indicate the model's proposed route.



Figure 13: Examples of successful shortest routes generated by o3 in the Shortest Route Navigation (SRN) task. Notes: due to space constraints, the Cartographic Maps are cropped from the original inputs. And, blue arrows are overlaid to indicate the model's proposed route.

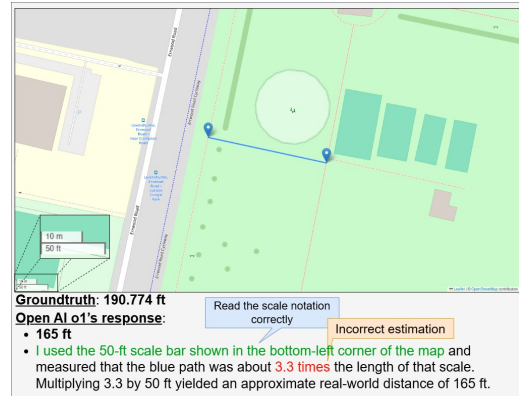


Figure 9: Example of OpenAI o1's response in the Route Length Estimation (RLE) task, demonstrating the ability of reading the scale notation but failing to correctly measure the path's length based on the scale unit.

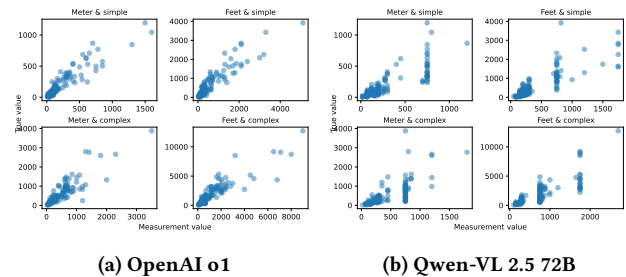


Figure 10: Scatter plots comparing model's proposed measurements with true route lengths in the RLE task.

Table 10: Comparison in performance between Single-Type Map Feature (STMF) and Multiple-Type Map Feature (MTMF) tasks, measured on STMF.

Model	STMF		MTMF	
	Counting ar^2 (\uparrow)	Name listing amF1 (\uparrow)	Counting ar^2 (\uparrow)	Name listing amF1 (\uparrow)
Llama 3.2 11B	0.143	0.342	-0.737	0.163
InternVL2.5 8B	0.095	0.407	-0.112	0.285
LlaVa-OV 7B	0.528	0.340	-0.167	0.109
QwenVL 2.5 7B	0.342	0.624	0.042	0.482
Llama 4 Scout	0.266	0.663	0.270	0.524
Llama 3.2 90B	0.312	0.542	-0.216	0.356
InternVL2.5 78B	0.618	0.519	0.289	0.455
LlaVa-OV 72B	0.490	0.537	-0.274	0.311
QwenVL 2.5 72B	0.401	0.706	0.311	0.610
GPT-4(V)	0.359	0.687	-0.166	0.491
GPT-4o	0.626	0.821	0.142	0.592
o1	0.581	0.813	0.486	0.791
o3	0.592	0.847	0.474	0.778
Gemini 2.5 Pro	0.761	0.894	0.584	0.808
Claude 3.7 Sonnet	0.624	0.714	0.520	0.633